J. Condensed Matter Nucl. Sci. 19 (2016) 264–273

Research Article

Investigation of Enhancement and Stimulation of DD-reaction Yields in Crystalline Deuterated Heterostructures at Low Energies using the HELIS Ion Accelerator

A.S. Rusetskiy*, A.V. Bagulya, O.D. Dalkarov, M.A. Negodaev and A.P. Chubenko

P.N. Lebedev Physical Institute (LPI), Russian Academy of Sciences, Leninskii pr. 53, Moscow 119991, Russia

B.F. Lyakhov and E.I. Saunin

A.N. Frumkin Institute of Physical Chemistry and Electrochemistry, Russian Academy of Sciences, Moscow 119071, Russia

V.G. Ralchenko

Prokhorov General Physics Institute, Russian Academy of Sciences, Moscow 119991, Russia

Abstract

In this study, we present the results of studies of DD reactions in crystalline heterostructures at low energies using the ion accelerator HELIS. The results of measurements of the DD-reaction yields from the Pd/PdO:D_x and the Ti/TiO_2:D_x heterostructures in the energy range of 10–25 keV are presented. The neutron and proton fluxes are measured using a neutron detector based on ^{3}He-counters and a CR-39 plastic track detector. Comparisons with calculations show significant DD-reaction yield enhancement. It was first shown that the impact of the H^+ and Ne^+ ion beams in the energy range of 10–25 keV at currents of 0.01–0.1 mA on the deuterated heterostructure results in an appreciable DD-reaction yield stimulation. We also studied the neutron yield in DD reactions within a polycrystalline deuterium-saturated CVD diamond, during irradiation of its surface by a deuterium ion beam with energy of less than 30 keV. The measurements of the neutron flux in the beam direction are performed in dependence on the target angle, β, with respect to the beam axis. A significant anisotropy in neutron yield is observed, it was higher by a factor of 3 at $\beta = 0$ compared to that at $\beta = \pm 45^\circ$.
 ISSN 2227-3123

Keywords: Enhancement of reaction yield, DD-reaction, Ion accelerator, Neutron detector, Plastic track detector

1. Introduction

The HELIS facility [1] at the P.N. Lebedev Physical Institute (LPI) operates with continuous ion beams with currents up to 40 mA and energies up to 50 keV. This multi-purpose accelerator addresses a wide spectrum of physics experiments,

*Corresponding author. E-mail: rusets@lebedev.ru

 ISSN 2227-3123

such as, e.g. light nuclei collisions at energies of several keV, investigation of elementary and collective processes in ion-beam plasma, and studies of the beam–target interactions using different materials with modification of the properties of the latter through ion-beam spattering of the thin-film coatings. In recent years, at HELIS, we studied the interactions of the deuterium beam with deuterium enriched crystalline heterostructures at energies of 10–25 keV.

Hitherto yields of DD-reaction in metal targets were studied mainly using only accelerators at energy $E_{\rm lab} \geq 2.5$ keV [2–7]. The desired further reduction of the accelerating voltage leads to serious problems related to the maintenance of current which makes it impossible to measure the products of the DD-reaction in a reasonable experiment duration, due to the extremely low yield. At the same time, a study of the behavior of yield (cross-section) DD-reaction at low energy deuterons (<1 keV) is of great interest in the study of processes and astrophysical screening effects in condensed media, leading to possible enhancement of the nuclear interaction of hydrogen isotopes in the metal.

Work [2] is very well known and frequently refereed, but the first results on dependence of DD-reaction yield on the target material was obtained in [3,4]. Experiments [8] demonstrated that the pulsed glow discharge capable of generating ions with energies of 0.8–2.5 keV and current densities of 300–600 mA/cm^2 at a deuterium pressure of 2–10 mm Hg. The current density used in the bombardment of the surface of the cathode (target) in a glow discharge is almost three orders of magnitude higher than that achieved with the use of accelerators. Analysis of the data showed that when $E_{\rm d} = 1.0$ keV Ti target bombarded by deuterons at a discharge current $I \sim 300$ mA, the gain of the reaction d(d,p)t was 10^9 in relation to the value of the yield at cross-section that defines the standard DD-reaction (approximation Bosch–Halle) [9]. Important factors that affect the enhancement of nuclear reactions in solids include a variety of external radiation (electrons, ions, X-rays, etc.). For example, in [10], it was shown that the effect of the electron beam with an energy of 30 keV and an X-ray beam with an energy up to 120 keV photons initiate in the systems Pd/PdO:D_x and Ti/TiO_2:D_x fusion of deuterium nuclei with the emission of 3 MeV protons.

Previous works [11–14] presented our results on dependence of DD-reaction yield on the target material and current beam density, as well as the results on enhancement of DD-reaction yield by ion beans.

2. Experimental Methods

2.1. HELIS facility

The HELIS facility (Fig. 1) is an ion accelerator of different gases to energy < 50 keV and includes: ion source with equipment, providing the power supply; beam focusing system; vacuum system; diagnostic apparatus for measuring current and ion beam energy.

2.2. Detector technology

Block diagram of the detector placement is shown in Fig. 2. A neutron detector based on ^{3}He-counters with organic glass and paraffin radiators is placed along and across the beam direction. CR-39 track detectors with various coatings surround the target irradiated by deuterium beam.

The CR-39 detector calibration by protons and alpha-particles was presented in [10]. The calibration of detectors 1 and 2 (placed along and above the sample) with the extended ^{238}Pu alpha source, simulating the sample position. Detection efficiency of CR-39 (in positions 1 and 2) to alpha-particles at 7 h etch was defined as $\varepsilon = 2.6\%$. The CR-39 detector was also calibrated by ^{252}Cf neutrons. Proton recoil spectrum after 7 h etch in 6 M NaOH at 70°C is at 4.5–8.0 μm track diameter (maximum at 5.2 μm) (Fig. 3). The neutron detection self-efficiency of CR-39 at 7 h etch was determined as $\varepsilon_{\rm n} \sim 10^{-4}$.

The ^{3}He detector was also calibrated by ^{252}Cf neutron source placed in the target position. The neutron detection efficiencies of ^{3}He detector groups at distance $R_1 = 85$ cm and $R_2 = 38$ cm were determined to be 0.1% and 0.4%, respectively.

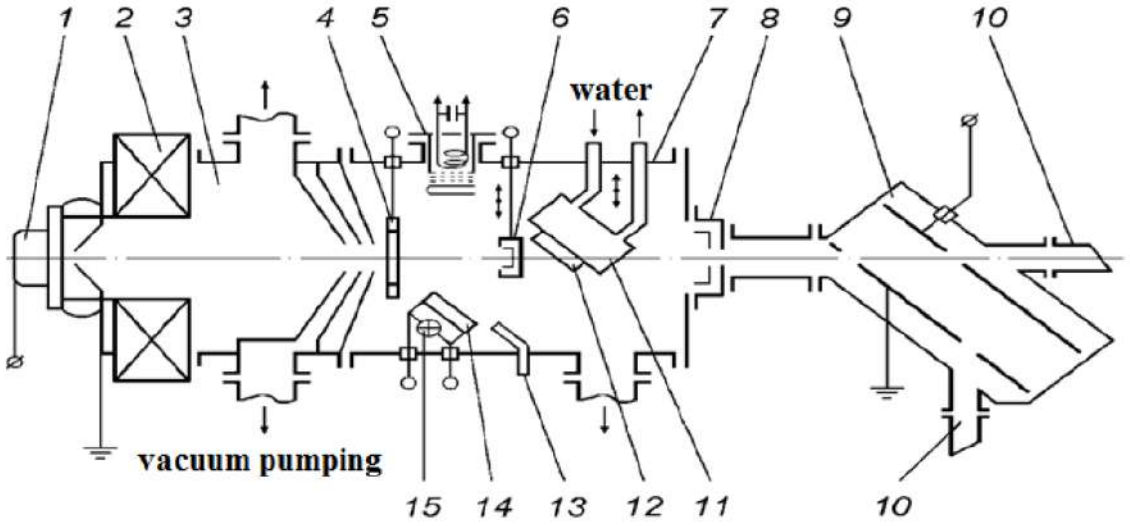

Figure 1. HELIS facility: 1 – ion source (duoplasmatron), 2 – electromagnetic lens, 3 – three-stage chamber of differential pumping, 4 – meter of a current of a transient-time type, 5 – auxiliary ion source, 6 – Faraday cap, 7 – chamber of targets, 8 – the device for calorimetric definition of a current of an ion beam, 9 – electrostatic analyzer, 10 – receivers of parsed fragments, 11 – water (or liquid gas)-cooled holder of the target, 12 – target, and 13 – feeder of gas in an vacuum chamber.

2.3. Pd and Ti sample preparation

The PdO/Pd/PdO samples were prepared by thermal oxidation from Pd foil (99.95% purity) of 50 μm thick with dimensions $S = 30 \times 10$ mm^2. Electrochemical loading in 0.3 M-LiOD solution in D_2O with Pt anode; $j = 10$ mA/cm^2. D/Pd ~ 0.73 (about 40 min required). The samples were rinsed in pure D_2O and were put in the Dewar glass to cool them down to 77 K. The cooled samples were then rapidly mounted (during ~ 1 min) in sample holder in front of CR-39 detectors set, placed into HELIS chamber, vacuumed and irradiated by D^+ beam.

The Ti foils of 30 and 300 μm thick were loaded in a 0.2 M solution of D_2SO_4 in D_2O over 36 h at 10 mA/cm^2, in order to dissolve the TiO_2 oxide layer at the Ti-surface and to provide D-penetration. The average loading (D/Ti = 0.1 at depth of ~ 1 μm) was determined by weight balance. Saturation of the sample can be carried out long before irradiation because the compound is absolutely stable at 300 K. The sample preparation procedure is described in more detail in [10].

2.4. The target of the polycrystalline diamond (CVD-diamond)

In our previous investigations of DD-reactions in the crystal targets (Pd, Ti), anisotropy was observed: the neutron flux along the beam direction was higher than that in the transverse direction [11,12]. This effect could be explained by the presence of narrow channels in the samples, where the bulk of deuterium, trapped during electrolysis, is concentrated. Particularly large anisotropy was observed using polycrystalline textured CVD diamond samples. The structure of the polycrystalline diamond film in cross section is shown in Fig. 4. The structure looks like columns growing from a few microns to about a hundred microns. More details about the CVD sample preparation procedure are described in [15]. The gaps between the columns are filled with deuterium atoms after electrolytic saturation.

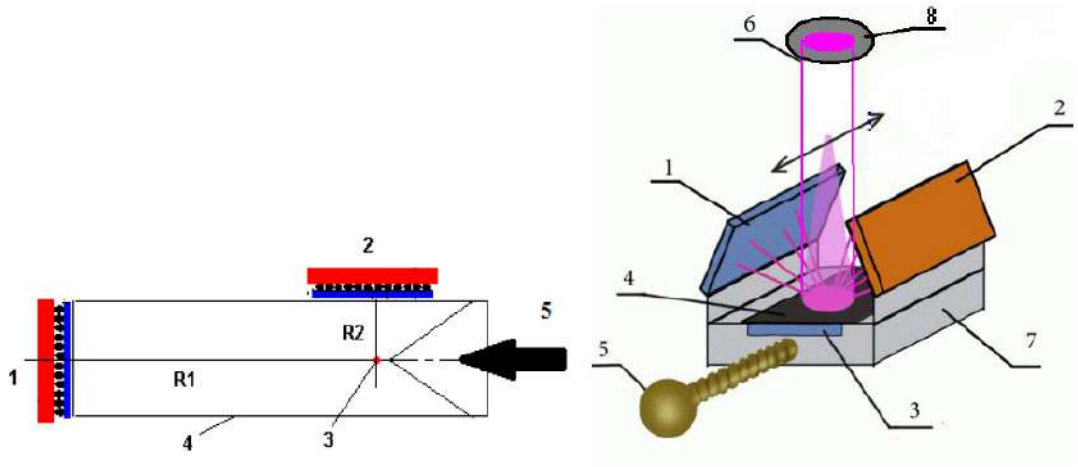

Figure 2. *Left panel*: the ^{3}He detector setup at HELIS, representing the first (1) and the second (2) ^{3}He-counter groups with radii $R_1 = 85$ cm and $R_2 = 38$ cm, respectively. The target is placed at (3) inside the HELIS beam pipe (4). The ion beam direction is indicated by (5). *Right panel*: Schematic representation of the target and track detector positions in the ion beam of the HELIS setup. (1)–(3) CR-39 track detectors with various coatings, (4) target, (5) manipulator, (6) ion beam, (7) water-cooled holder of the target, and (8) diaphragm.

3. Experimental Results

Thick target DD-reaction yield calculated using formula (1).

$$Y_{\mathrm{DD\,a.u.}} = Y_{\mathrm{DD}}/J_{\mathrm{d}} = N_{\mathrm{eff}}(T) \times \int_0^{E_{\mathrm{d}}} \sigma_{\mathrm{DD}}(E)(\mathrm{d}E/\mathrm{d}x)^{-1}\mathrm{d}E, \tag{1}$$

where Y_{DD} is the DD-reaction intensity, J_{d} the deuteron current; $N_{\mathrm{eff}}(T)$ the effective concentration of bounded D in metal at temperature T, captured at depth x:

$$N_{\mathrm{eff}}(T) = N_0\ \exp(-\varepsilon_{\mathrm{d}}\Delta T/k_{\mathrm{B}}T\,T_0),$$

where N_0 is the D concentration at $T_0 = 290$ K, ε_{d} the deuteron activation energy, k_{B} the Boltzmann constant, σ_{DD} the "bare" DD- cross-section, and $\mathrm{d}E/\mathrm{d}x$ is the stopping power in target calculated with Monte-Carlo code SRIM [16].

$$f(E) = Y_{\mathrm{exp}}E)/Y_{\mathrm{b}}(E) = \exp[\pi\eta(E)U_{\mathrm{e}}E]\ \ -\ \text{enhancement factor},$$

where $Y_{\mathrm{exp}}(E)$ is the experimental yield of DD-protons, $Y_{\mathrm{b}}(E)$ is the yield at the same energy, determined according to the Bosch & Halle extrapolation, and $2\pi\eta = 31.29Z^2(\mu/E)^{1/2}$ is the Sommerfeld parameter (where Z is the deuteron charge, μ and E are the reduced deuteron mass and energy, respectively). U_{e} is the screening potential.

3.1. Ti/TiO_2:D_x target and Pd/PdO:D_x under the D^+ beam

The energy dependence of the fluxes of protons and neutrons emitted along and opposite to the beam for Ti/TiO_2:D_x and Pd/PdO:D_x targets is shown in Fig. 5. There is the anisotropy in the escape of DD-reaction products emitted along

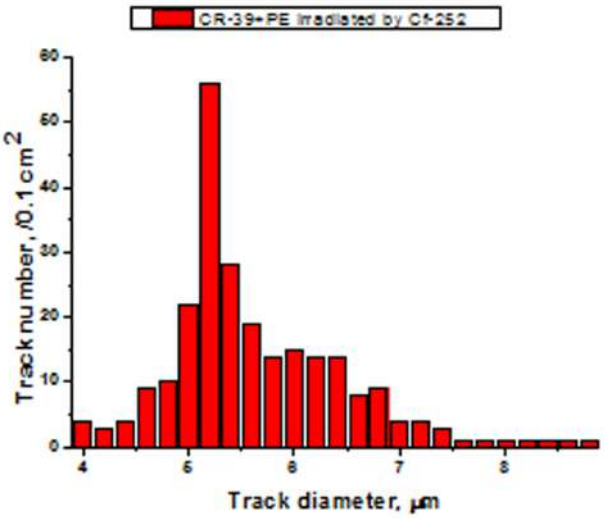

Figure 3. Proton recoil spectrum of CR-39 after 7 h etch in 6 M NaOH at 70°C.

and opposite to the beam. The dependence of the DD-reaction yield from the Ti/TiO_2:D_x and Pd/PdO:D_x target on the deuteron energy and the DD-reaction yields calculated by (1) for the given experimental conditions are shown in Fig. 6.

Accurate measurement of the temperature on the target is a difficult technical problem. The screening potentials were calculated for two "extreme" conditions:

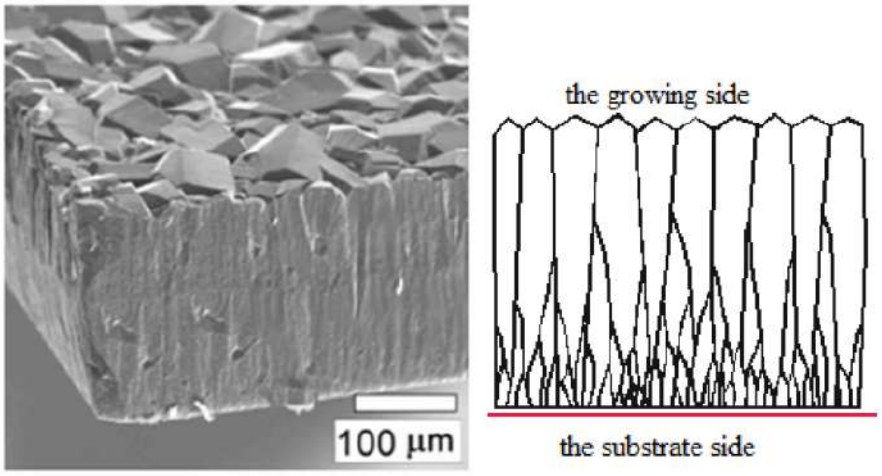

Figure 4. The structure of the polycrystalline textured diamond film in cross section.

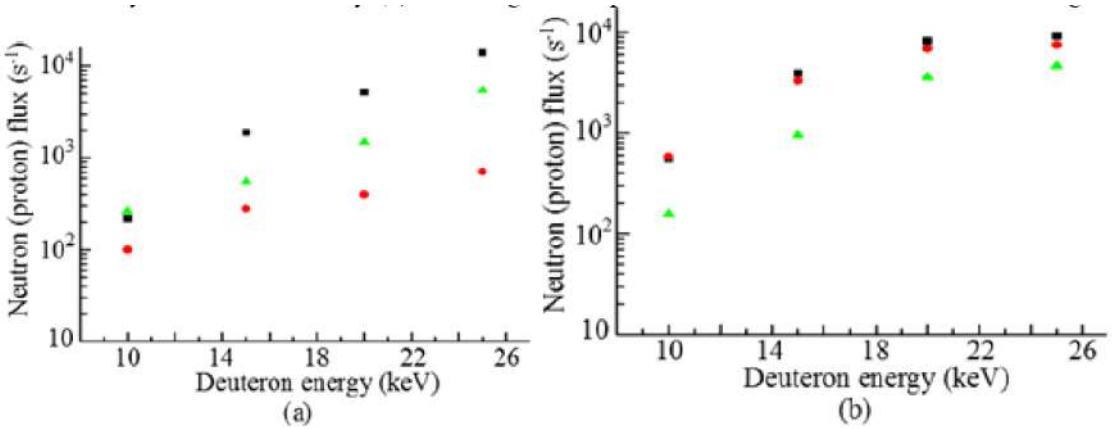

Figure 5. The energy dependence of the fluxes of protons and neutrons emitted along and opposite to the beam for Ti/TiO_2:D_x(left) and Pd/PdO:D_x (right) targets. Neutron flux along the beam (■), neutron flux opposite to the beam (red filled circles), and proton flux opposite to the beam (green filled triangles). Measurements were performed by the CR-39 track detector.

(1) at $T = T_{\rm m}$, i.e., the metal melting temperature in the beam region, and
(2) at 350 K, i.e., the temperature measured by a thermocouple at the target edge.

Comparison with calculations shows significant effects of DD-reaction yield enhancement. The screening potential for Pd/PdO:D_x heterostructure under experimental conditions was estimated as $U_{\rm e} = 630 - 980$ eV. The screening potential for Ti/TiO_2:D_x heterostructure under experimental conditions was estimated to be in the range $U_{\rm e} = 160 - 750$ eV [11,12].

3.2. Ti/TiO_2:D_x target and Pd/PdO:D_x under the H^+ and Ne^+ beam

We studied the possibility of stimulating the DD-reaction yield from the Ti/TiO_2:D_x and the Pd/PdO:D_x heterostructures by ion beams using the HELIS setup. Instead of the deuteron beam, we used H^+ and Ne^+ ion beams in the

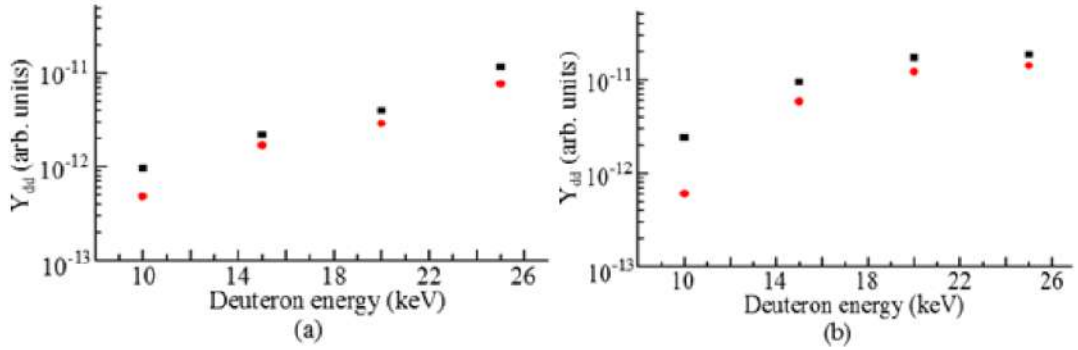

Figure 6. Dependence of the DD-reaction yield from the Ti/TiO_2:D_x target (left) and from the Pd/PdO:D_x target (right) on the D^+ beam energy: the measured DD-reaction yield along the beam (■) and the DD-reaction yield calculated for a given energy (red filled circles).

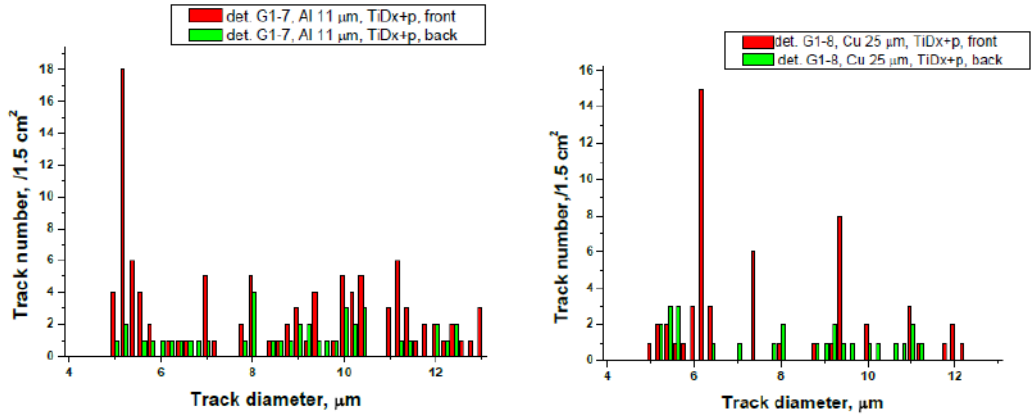

Figure 7. Diameter distribution of tracks on the detectors coated 11 μm Al (left) and 25 μm Cu (right), located above the sample Ti/TiO_2:D_x, irradiated by a H^+ beam with an energy of 23 keV. Comparison of readings front and back sides of the detectors indicates the presence of proton emission from the DD-reaction.

energy range of 10–25 keV to irradiate the Ti and Pd deuterated targets. Comparison of readings from the front and back sides of the CR-39 detectors placed over the target indicates the presence of proton emission from the DD-reaction – left peak in diameter distributions (see Fig. 7). Comparison of readings from the front and back sides of the CR-39 detectors under the target indicates the presence of neutron emission from the DD-reaction (Fig. 8).

Figure 9 shows the results of neutron flux measurements by the ^{3}He detector under the action of H^+ and Ne^+ beams on the Ti/TiO_2:D_x target. Background measurements were performed with similar beams on the Cu target. We can see that the beam exposure of the Ti/TiO_2:D_x target causes an increase in neutron detector indications over background values. Results obtained were similar in stimulating the target Pd/PdO:D_x beams of H^+ and Ne^+ [13,14].

To estimate the DD-reaction yields from targets during irradiation with the ion beam, we used a simplified model

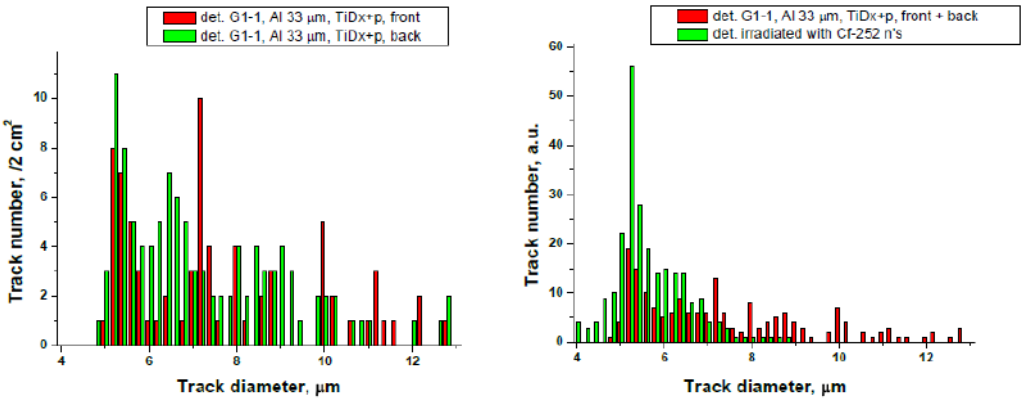

Figure 8. *Left* - the diameter distribution of the tracks on the front (red bars) and rear (green bars) side of the detector coated 33 mm Al, located below the sample Ti / TiO_2: D_x, irradiated by a proton beam with an energy of 23 keV. *Right* - Total tracks diameter distribution of the front and rear sides of the detector (red columns) compared with a detector irradiated by neutrons from the source Cf-252 (green bars).

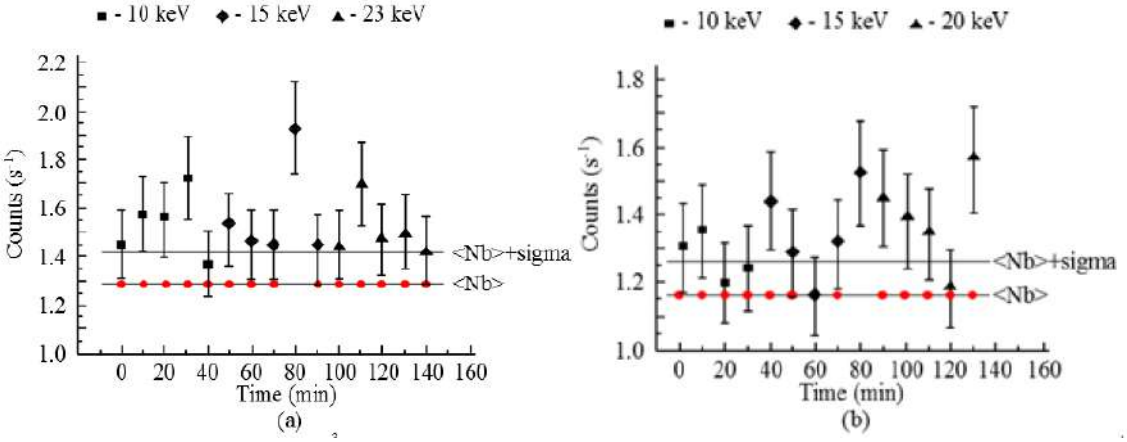

Figure 9. Counting rate of the ^{3}He-neutron detector (■, ♦, ▲). (a) Ti/TiO_2:D_x target 300 μm thick and H^+ beam (10, 15, and 23 keV), (b) Ti/TiO_2:D_x target 30 μm thick and Ne^+ beam (10, 15, and 20 keV). The average background $\langle$Nb$\rangle$ (red filled circles) was measured using the Cu target.

of the process, taking into account that deuterium desorption stimulated by radiation cause a deuteron current moving to the surface from the sample. This deuteron current and the deuterated surface can be considered the beam and target, respectively.

The screening potential U_e was estimated by the semi-empirical formula [17]

$$U_\mathrm{e} = (T/T_0)^{-1/2}[a\ln(y) + b], \tag{2}$$

where $a = 145.3$ and $b = 71.2$ are numerical constants and $y = k \times y_0(J_\mathrm{d}/J_0)$, here $k = \exp(-\varepsilon_\mathrm{d}\Delta T/k_\mathrm{B}T\,T_0), \varepsilon_\mathrm{d}$ is the deuteron activation energy, $y_0 =$ Me/D is the concentration ratio of metal and deuterium atoms in the target at $T_0 = 290$ K and $J_0 = 0.03$ mA/cm^2, and J_d is the deuteron current density from the target. The deuteron current was determined by the deuterium desorption rate from the sample.

- The screening potential for the Pd/PdO:D_x target, calculated using formula (2), is $U_\mathrm{e} = 897$ eV.
- The screening potential for the Ti/TiO_2:D_x target, calculated using formula (2), is $U_\mathrm{e} = 796$ eV.

3.3. CVD diamond target under the D^+ beam

In our previous investigations of DD-reaction in the crystal targets (Pd,Ti), anisotropy was observed: the neutron flux along the beam direction was higher than that in the transverse direction. This effect could be explained by presence of narrow channels in the samples, where the bulk of deuterium, trapped during the electrolysis, is concentrated. Particularly large anisotropy was observed using a polycrystalline textured CVD diamond samples.

We investigated the dependence of the DD-reaction yield from the incidence angle of the beam on the target. The relative yield of the DD reaction $Y_\mathrm{dd} = n_\mathrm{n}/(S \times I_\mathrm{d})$, where n_n is the longitudinal or transverse neutron flux, S the irradiated area of the target, and I_d is the ion beam current.

The measurements of the neutron flux in the beam direction are performed in dependence on the target angle, β, with respect to the beam axis. A significant anisotropy in neutron yield is observed, it was higher by a factor of 3 at $\beta = 0°$ compared to that at $\beta = \pm 45°$ NC-20 (80% of diamond, 20% of graphite) is composite material with

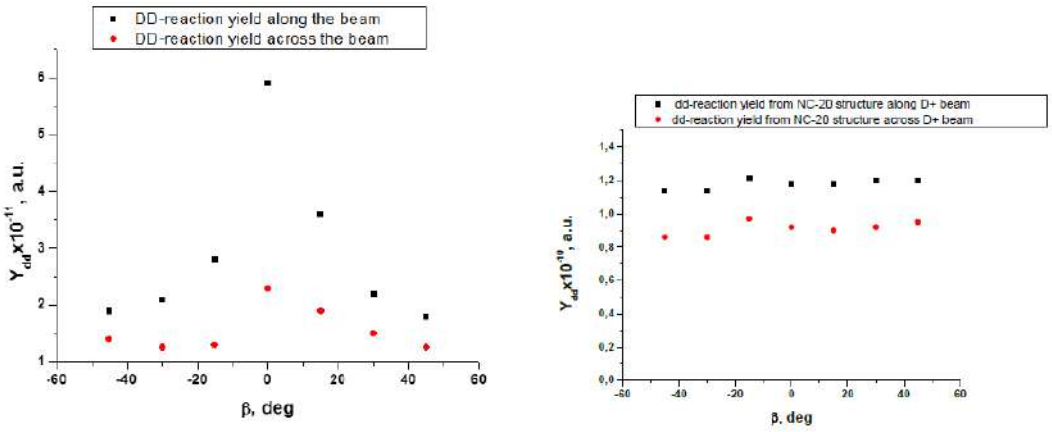

Figure 10. *Left* - The neutron yield obtained with the textured CVD-diamond sample as a function of the angle between the beam and the target plane norm, measured longitudinally (black filed squares) and transverse (red filled diamonds) directions with respect to the ion beam. Ion beam with the energy of $E_{\rm d} = 20$ keV and the current of 50–60 mA. *Right* – The neutron yield obtained with the diamond composite material (NC-20) as a function of the angle between the beam and the target plane norm, measured longitudinally (black filled squares) and transverse (red filled diamonds) directions with respect to the ion beam. NC-20 (80% of diamond, 20% of carbon) is composite material with isotropic structure. Ion beam with the energy of $E_{\rm d} = 25$ keV and the current of 20 mA.

isotropic structure. It was observed, that the neutron yield from isotropic NC-20 sample was practically independent of the sample orientation with respect to the beam (see Fig. 10).

Possible reasons for the increasing of DD-reaction yield in textured CVD diamond include the following:

- Screening effects of deuterium nuclei in the crystal structure.
- Collective processes associated with a high concentration of deuterium in certain directions.
- The effects of channeling, leading to an increase in the effective range of ions in the direction of the channel.

The results were presented in CHANNELING 2014 (Capri (Napoli), Italy, October 5–10, 2014) and published in [18].

4. Conclusions

The results of measurements of the DD-reaction yields from the Pd/PdO:D_x and the Ti/TiO_2:D_x heterostructures in the energy range of 10–25 keV show a significant effect of DD-reaction yield enhancement.

It was first shown that the impact of the H^+ and Ne^+ ion beams in the energy range of 10–25 keV at currents of 0.01–0.1 mA on the deuterated heterostructures results in the appreciable DD-reaction yield stimulation and enhancement.

It was observed that the crystalline structure and the orientation of the sample with respect to the beam has an impact on the neutron yield. The highest yield is recorded with the textured CVD-diamond target, oriented perpendicular to the beam.

Acknowledgements

This work was supported by the Russian Ministry of Education and Science (No. 16.518.11.7104 government contracts from 27 October 2011 and No. 14.518.11.7075 from18 June 2013.) The authors are very grateful to S.S. Gershtein and G.A. Mesyats for fruitful discussions.

References

[1] A.S. Roussetski, M.N. Negodaev and A.G. Lipson, *Proc. of ICCF15,* 5–9 Oct. 2009, Rome, Italy, p.182.
[2] F. Raiola, P. Migliardi, L. Gang et al., *Phys. Lett.* **B547** (2002) 193.
[3] H. Yuki, J. Kasagi, A.G. Lipson et al., *JETP Lett.* **68** (1998) 785.
[4] H. Yuki, T. Sato, J. Kasagi et al., *J. Phys. G: Nucl. Part. Phys.* **23** (1989) 1459.
[5] M. Aliotta, F. Raiola, G. Gyurky et al., *Nucl. Phys.* **A690** (2001) 790.
[6] K. Czerski, A. Hulke, A. Biller et al., *Europhys. Lett.* 54 (2001) 449.
[7] F. Raiola, P. Migliardi, G. Gyurky et al., *Euro. Physical J*. **A13** (2002) 377.
[8] A.G. Lipson, A.S. Roussetski, A.B. Karabut and G.H. Miley, *JETP* **100** (2005) 1175.
[9] H.S. Bosch and G.M. Halle, *Nucl. Fusion* **32** (1994) 611.
[10] I. P. Chernov, A. S. Rusetskii, D. N. Krasnov et al., *JETP* **112**(6) (2011) 952–960.
[11] A.V. Bagulya, O.D. Dalkarov, M.A. Negodaev, A.S. Rusetskii and A.P. Chubenko, *Bulletin Lebedev Physics Institute* **39** (9) (2012) 247–253.
[12] A.V. Bagulya, O.D. Dalkarov, M.A. Negodaev, A.S. Rusetskii and A.P. Chubenko, *Bulletin Lebedev Physics Institute* **39**(12) (2012) 325–329.
[13] A.V. Bagulya, O.D. Dalkarov, M.A. Negodaev, A.S. Rusetskii, A.P. Chubenko and A.L. Shchepetov, *Bulletin Lebedev Physics Institute* **40**(10) (2013) 282–284.
[14] A.V. Bagulya, O.D. Dalkarov, M.A. Negodaev, A.S. Rusetskii, A.P. Chubenko and A.L. Shchepetov, *Bulletin of the Lebedev Physics Institute* **40**(11) (2013) 305–309.
[15] V.G. Ralchenko, E. Pleuler, F.X. Lu, D.N. Sovyk, A.P. Bolshakov, S.B. Guo, W.Z.Tang, I.V. Gontar, A.A. Khomich, E.V. Zavedeev and V.I. Konov, *Diamond and Related Materials* **23** (2012) 172–177.
[16] J.F. Ziegler and J.P. Biersack, code SRIM 2003.
[17] A.G. Lipson, A.Yu. Tsivadze, B.F. Lyakhov, E.I. Saunin, D.M. Sakov, I.P. Chernov, Yu.P. Cherdantsev, Yu.I. Tyurin and A.S. Rusetskii, *Doklady Physics* **54**(4) (2009) 182–186.
[18] A.V. Bagulya, O.D. Dalkarov, M.A. Negodaev, A.S. Rusetskii et al., *Nucl Instr Methods Phys Res* B **355** (2015) 340–343.